

Inactivation of airborne viruses using a packed bed non-thermal plasma reactor

T Xia^{1,3} , A Kleinheksel¹, E M Lee², Z Qiao¹, K R Wigginton¹ and H L Clack¹

¹ Department of Civil and Environmental Engineering, University of Michigan, Ann Arbor, MI, United States of America

² Department of Mechanical, Materials, and Aerospace Engineering, Illinois Institute of Technology, Chicago, IL, United States of America

E-mail: xiatian@umich.edu

Received 28 November 2018, revised 25 March 2019

Accepted for publication 28 March 2019

Published 23 April 2019




CrossMark

Abstract

Outbreaks of airborne infectious diseases such as measles or severe acute respiratory syndrome can cause significant public alarm. Where ventilation systems facilitate disease transmission to humans or animals, there exists a need for control measures that provide effective protection while imposing minimal pressure differential. In the present study, viral aerosols in an airstream were subjected to non-thermal plasma (NTP) exposure within a packed-bed dielectric barrier discharge reactor. Comparisons of plaque assays before and after NTP treatment found exponentially increasing inactivation of aerosolized MS2 phage with increasing applied voltage. At 30 kV and an air flow rate of 170 standard liters per minute, a greater than 2.3 log reduction of infective virus was achieved across the reactor. This reduction represented ~ 2 log of the MS2 inactivated and ~ 0.35 log physically removed in the packed bed. Increasing the air flow rate from 170 to 330 liters per minute did not significantly impact virus inactivation effectiveness. Activated carbon-based ozone filters greatly reduced residual ozone, in some cases down to background levels, while adding less than 20 Pa pressure differential to the 45 Pa differential pressure across the packed bed at the flow rate of 170 standard liters per minute.

Keywords: non-thermal plasma, bioaerosol inactivation, bacteriophage MS2, ozone, plaque assay, qPCR

 Supplementary material for this article is available [online](#)

(Some figures may appear in colour only in the online journal)

Introduction

Airborne infectious disease outbreaks such as measles, tuberculosis, and severe acute respiratory syndrome (SARS) can cause risk of infection by the essential and involuntary action of respiration. Airborne disease transmission, the processes governing it, and the development of protective measures against it, are less understood than transmission via water, food, arthropod vectors, and direct contact with infected individuals. Disease transmission among humans and animals often involves either direct contact with an infected individual or transport across

very short distances; however, pathogen transmission over longer distances can also occur. The SARS outbreak within the Amoy Gardens housing complex in Hong Kong [1] was spread between apartments by sewer main gases drawn in by improperly sized ventilation fans and poorly maintained drains.

Livestock diseases such as Newcastle disease, avian influenza, hoof-and-mouth disease, porcine reproductive and respiratory syndrome (PRRS), and African swine flu are potential threats to global food security. In pork and poultry production, biosecurity measures for preventing the introduction of pathogens into animal confinement buildings primarily protect against disease spread through direct contact between animals and from pathogen-contaminated surfaces. PRRS and avian

³ Author to whom any correspondence should be addressed.

and porcine influenza are two examples of high impact diseases for which biosecurity measures have been implemented to prevent airborne transmission. The virus that causes PRRS is understood to survive transmission through the atmosphere in greater numbers when atmospheric conditions are cool, damp, or cloudy [2]. Long-term changes in climate and their influences on infectious disease outbreaks vary by route of transmission and are highly uncertain [3]. While increasing vector populations with increasing annual average temperature and precipitation could increase vector-borne transmission, the influences of changing meteorological conditions on airborne transmission of pathogens are unclear.

In contexts where humans or animals move freely, the potential for disease transmission through direct contact is greater, reducing the importance of airborne transmission and greatly limiting the utility of airborne pathogen inactivation. However, where airborne transmission is or is suspected of being an important transmission route, few mitigation technologies exist. Disinfection by UV irradiation requires UV doses involving a combination of radiative fluxes and exposure times that have been established [4], which are difficult to implement in air. Upper-room UV irradiation relies on natural air circulation patterns within a room to transport airborne pathogens into the illumination zone of a wall-mounted, upward facing UV fixture near the ceiling. Upper room UV was proven effective in reducing TB transmission in hospital wards [5] and rubella transmission within army barracks [6]. UV germicidal irradiation (UVGI) directs UV radiation onto conventional particulate filters within ventilation systems to inactivate bacteria and viruses captured on the filter surfaces [7]; however, viruses and bacteria that migrate into the filter media or that are shielded from the UV source as subsequent particles are collected, are inactivated with lower efficiencies [7]. The US EPA concludes that there is insufficient evidence, and no standard test procedures, for assessing UVGI performance and that UVGI provides virtually no additional protection over the use of conventional HEPA filtration alone [8]. Conventional filtration presents several drawbacks, including the low fluid permeability needed for high particle collection efficiency, which inherently increases the differential pressure across the filter and promotes infiltration of untreated air into indoor spaces at partial vacuum. In buildings not constructed to an air-tight standard, this can lead to high costs of building reconstruction and retrofit.

Two factors govern the potential for disease transmission of airborne pathogens such as viruses and bacteria: aerosol transport and aerosol infectivity [9]. UV radiation alone only addresses aerosol infectivity and particle filtration only addresses aerosol transport. Unlike filtration and UV irradiation, non-thermal plasmas (NTPs) can address *both* transport (by charge-driven filtration) and infectivity (by reaction with reactive plasma species) of airborne pathogens. NTP is a result of electrical discharges within a neutral gas under atmospheric conditions and mainly consists of electrons, ions, and radicals. Unlike thermal plasma, where all constituents are in thermal equilibrium, a NTP in comparison is always in a state of non-equilibrium because the electrons with very light masses can reach higher temperatures (10^4 – 2.5×10^5 K) and attain higher kinetic energy (1–20 eV) than the rest of

the NTP constituents, which are heavier and at lower temperatures [10]. On these bases, an NTP is also known as non-equilibrium plasma or cold plasma. A commonly applied NTP reactor type is the dielectric barrier discharge (DBD) reactor. DBD or silent discharge refers to the electrical discharge through a dielectric barrier, such as glass, quartz, or alumina. A high voltage AC source is commonly used in a DBD reactor, because the changing polarity of AC is essential to sustain the electrical discharge in a DBD reactor. The dominant electrical discharge mode in a DBD reactor is microdischarge, which is in a form of filaments with nanosecond lifespan. When the microdischarge reaches a dielectric barrier, the dielectric surface allows for the spreading and accumulation of the charges and thus reduces the electric field until the field is completely quenched. The use of an AC source repeats the cycle by generating microdischarge with a different electrical polarity. In studying the effectiveness of removing air pollutants such as methyl tert-butyl ether (MTBE) by NTP, Holzer *et al* [11] utilized a gaseous plasma generated by a DBD reactor using different dielectric barriers including glass, Al_2O_3 , and TiO_2 . Kuwahara *et al* [12] developed a DBD reactor using polyester-laminated electrodes to evaluate the removal characteristics of odorous compounds, including NH_3 and NH_3 mixed with CH_3CHO , by NTP. In studying oil mist-to-gas conversion, Park *et al* [13] developed a DBD reactor using thin copper electrodes (0.05 mm thickness) where each electrode was sandwiched in between by two dielectric plates made of alumina (1 mm thickness).

A packed-bed reactor provides a more efficient way of treating trace air pollutants by adding pellets between the electrodes in a corona reactor or a DBD reactor. A typical air pollutant has a concentration in the range of parts per million by volume (ppmv), so direct interactions between the electrons and air pollutants are usually negligible under ambient conditions [10]. In a packed-bed reactor, the electron-impact reactions serve as the main plasma chemistry for air pollutant decomposition [14]. By packing the pellets, electron generation takes place through partial discharges at the pellet contact points within a packed-bed reactor. More specifically, an external electric field applied between the pellets and the electrodes enables polarization, which in turn induces partial discharges and subsequently the electron-impact reactions. While a packed-bed arrangement can provide evenly distributed flows, it can also lead to a higher pressure drop across the packed-bed. Perovskite pellets, such as BaTiO_3 and Al_2O_3 are commonly used dielectric materials for packed-bed reactors. The addition of catalytically active materials can further improve the selectivity of a packed-bed reactor. Mizuno *et al* [15, 16] discovered that a ferroelectric pellet packed-bed reactor was not only capable of collecting particles, but also destroying yeast cells. In studying organic solvents (e.g. MTBE, toluene, and acetone), Holzer *et al* [11] evaluated three packed-bed materials (i.e. glass beads, BaTiO_3 , and PbZrO_3 – PbTiO_3) and one catalyst (i.e. LaCoO_3) using various cylindrical DBD reactors designs, which showed that the ferroelectric packed-bed reactor using BaTiO_3 pellets significantly increased the conversion of MTBE and toluene to CO_x . Kuwahara *et al* [12] used a ferroelectric packed-bed reactor

to study the decomposition of odorous compounds (i.e. NH_3) by adding BaTiO_3 pellets to the previously developed DBD reactor, which used polyester-laminated electrodes. The results showed that the DBD reactor with ferroelectric packed-bed pellets could decompose NH_3 at a much faster rate than the DBD reactor alone.

Researchers [17, 18] have reported reductions in infective airborne pathogen concentrations as a result of NTP treatment, results that included confounding effects of extended exposure of viral aerosols to ozone [17] or loss of viral aerosols by charge-driven filtration [18]. In one study, a DBD NTP reactor with 10 s plasma exposure and a very high air flow rate (25 l s^{-1}) resulted in 97% *Escherichia coli* inactivation [17]. The research group found that the synergetic action of short-living plasma agents, such as hydroxyl radicals, and plasma-generated ozone, achieved the previously measured 97% in-flight inactivation of aerosolized *E. coli* [19]. Another research group constructed a 12 mm diameter DBD NTP device and reported >95% inactivation of bacteria and 85%–98% inactivation of fungal species with a 24 W reactor energy output and a flow rate of 28.3 LPM (liters per minute) [20]. That same team examined NTP inactivation of MS2 and reported over 95% MS2 airstream inactivation with a 28 W reactor energy output at 12.5 LPM flow rate [18]. None of these research, however, examined the airstream inactivation performance of a reactor with a pack-bed feature.

In this study, we describe the development and performance of a packed-bed NTP in-flight airstream disinfection process. A DBD NTP reactor was constructed to treat an air stream seeded with viral aerosols. Aerosols of bacteriophage MS2 were generated by the evaporation of fine mists produced by ultrasonic atomization. Plaque assay and quantitative polymerase chain reaction (qPCR) analyses were conducted to determine the abundance of infective and total MS2 aerosols, respectively, in the pre- and post-treatment samples. Ultimately, the ability to remove residual ozone with carbon filters was assessed. A maximum of 2.3 log reduction of infective MS2 virus was achieved by the reactor, demonstrating NTP is a viable technology for in-flight disinfection and the prevention of airborne virus transmission.

Materials and methods

Experimental setup

The experimental apparatus (figure 1) for NTP inactivation of viral aerosols includes: (1) an induced draft (ID) fan, (2) a DBD reactor, (3) an aerosol generator, (4) a digital oscilloscope, (5) a high voltage amplifier, and (6) a digital function generator. The aerosol generator is a modified consumer-grade cool-mist humidifier (Vicks V5100-N) that piezoelectrically atomizes virus buffer solution containing MS2, a single-stranded RNA bacteriophage. A 10.2 cm (4-inch) ID fan at the end of the apparatus draws ambient air (25%–36% RH) into a flexible duct (8.9 cm (3.5-inch) ID and 4 m (13-ft) length), where mixing occurs between the air and the droplets, allowing for droplet evaporation and thus bioaerosol generation. The droplet evaporation process is further enhanced by

the addition of a facility-supplied stream of dry compressed air (<10% RH; figure 1). The DBD reactor is powered by one of the two AC voltage amplifiers, namely a variable 0 to 20 kV (peak-to-peak) high voltage amplifier (Trek Model-610E) and a 30 kV neon transformer (France 15030 P5G-2UE ServiceMaster). The variable 0 to 20 kV high voltage amplifier is coupled with a digital function generator (BK Precision Model-4052), which outputs 60 Hz sinusoidal AC voltage. The amplifier can output applied voltage (U) signals at 1 V/1000 V and two current (I) signals, total current and return current, at 1 V/200 μA , which can be monitored directly by a digital oscilloscope (BK Precision Model-2190D). For the 30 kV neon transformer, a high voltage probe (Cal Test Electronics CT2700, 1 V/1000 V) and a Pearson current coil (Model 6585, 1V/1A) are connected to one of the power supply's high voltage electrodes (the schematic is illustrated in figure S1 in the supplementary information, available online (stacks.iop.org/JPhysD/52/255201/mmedia)), whose output signals are monitored by the digital oscilloscope. The power (P) of the reactor was therefore calculated according to the equation:

$$P = \frac{1}{T} \int_T U \times Idt \quad (1)$$

where T is the period of the AC voltage. A honeycomb-structured ozone filter (figure 1; Burnett Process Inc. BP-4810) is located downstream of the reactor to remove ozone from the exhaust. Two impingers installed upstream and downstream (figure 1) of the reactor enabled the quantification of virus inactivation by the NTP reactor.

NTP and reactor design

The NTP reactor developed in the present study utilizes the characteristics of DBD and packed-bed discharge for the application of viral aerosol inactivation. Figure 2 is a close-up schematic of the DBD packed-bed reactor. The reactor is composed of one larger Plexiglas tube (10.2 cm (4-inch) OD, 9.5 cm (3.75-inch) ID, 20.3 cm (8-inch) length) and two smaller tubes (8.9 cm (3.5-inch) OD, 7.6 cm (3-inch) ID, 30.5 cm (12-inch) length). The smaller tubes slide freely relative to the larger tube due to a clearance of 0.3 cm (0.125-inch). Two rubber O-rings, which sit in the grooves on the OD of the smaller tube permit an air-tight sliding mechanism. As indicated in figure 2, a circular perforated brass plate is installed at the end of each sliding tube to serve as the ground electrode and to evenly distribute the inlet and outlet flow of the reactor. The design of the sliding electrode allows for packed bed depth adjustment ranging between 0.6 and 12.7 cm (0.25 and 6 inches). A brass ring (0.9 mm (0.035-inch) thickness, 2.5 cm (1-inch) width) adhered to the OD of the larger Plexiglas tube serves as the high voltage electrode for the AC high voltage supply. Two flow plugs made of styrofoam (6.35 cm (2.5-inch) OD) are positioned at the center of the reactor to direct the airflow with viral aerosols through an annular region in which the plasma is concentrated (figure 2). The DBD reactor utilizes the microdischarge generated through a dielectric barrier made of Plexiglas. The packed-bed, consisting of 500 inert borosilicate glass beads (0.6 cm (0.25-inch) diameter), further

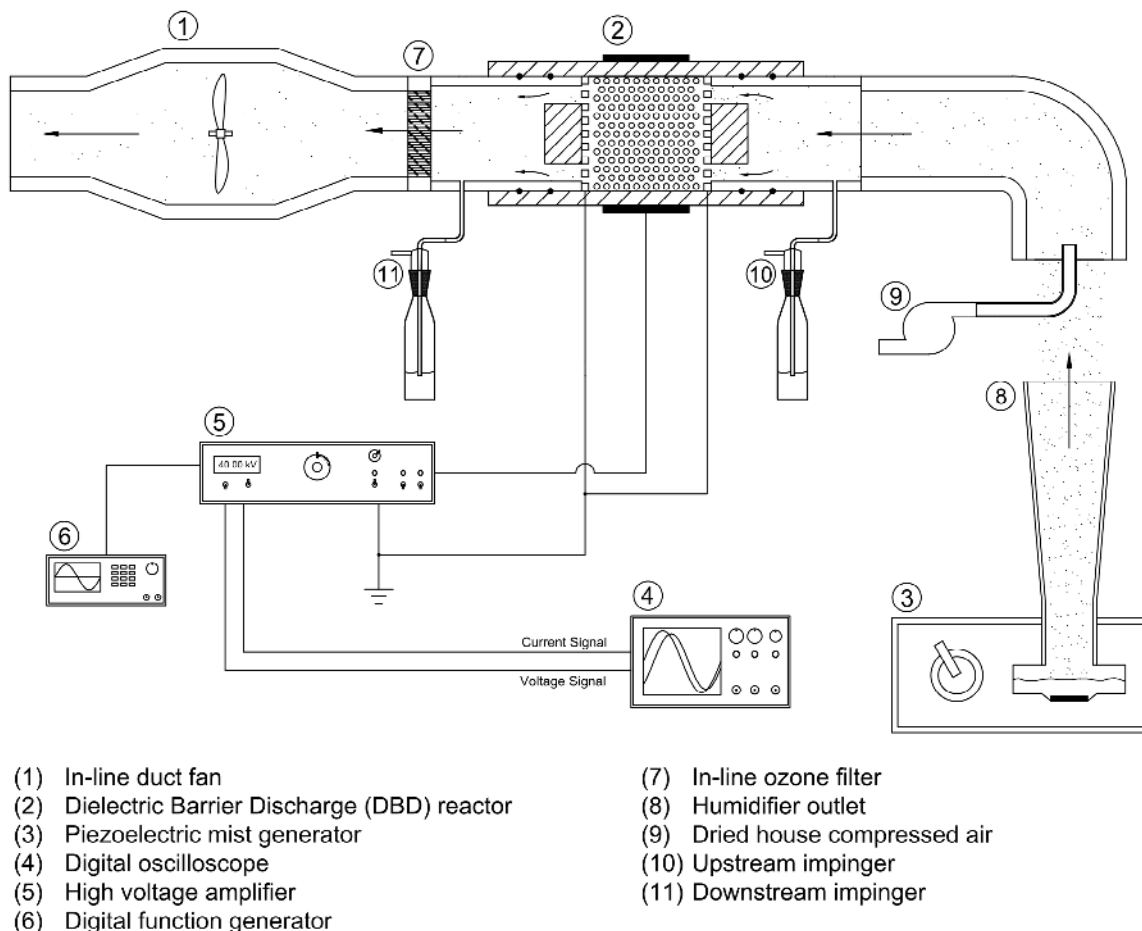


Figure 1. Experimental setup for the inactivation of viral aerosols with the 0–20kV variable amplifier.

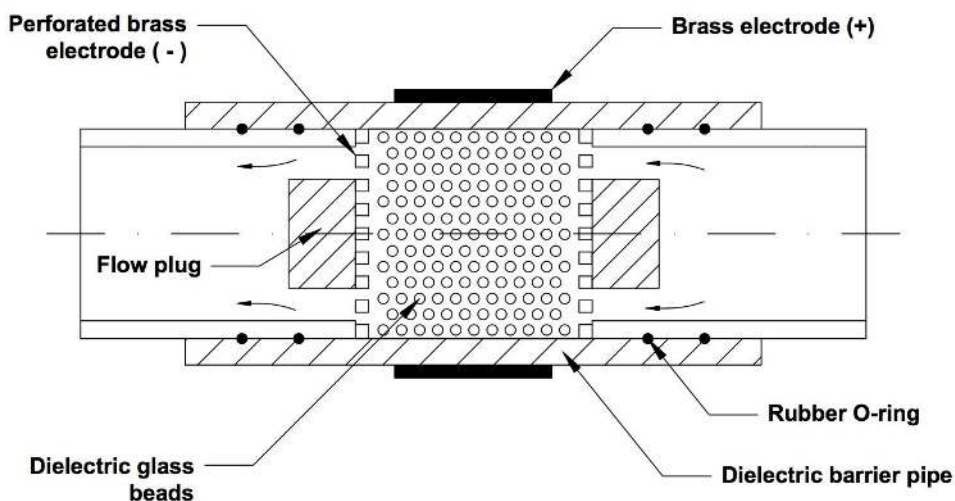


Figure 2. Schematic of the DBD packed-bed reactor.

enhances the microdischarge by partial discharges at the contact points between the glass beads for effective electron-viral aerosol collisions and inactivation process.

Experimental procedure

During the virus inactivation tests, a consumer-grade ultrasonic humidifier was used to generate MS2 viral aerosols from

the original virus solution. Each inactivation test involved adding 300 ml (for a 60 min test) or 200 ml (for a 30 min test) of MS2 solution consisting of $\sim 1 \times 10^8$ pfu ml⁻¹ in phosphate-buffered saline (PBS; 0.78 g NaH₂PO₄/L, 0.58 g NaCl/L, pH of 7.5) into the ultrasonic humidifier reservoir. The humidifier was set to built-in power level 2 (labeled as H2) and the atomization rate was approximately 117 ml h⁻¹ over a 30 min experimental period [21]. The air flow rate through

the sampling train was maintained by the ID fan with a viable transformer (Staco Energy 3PN221B). In each test, the ID fan and humidifier were turned on for five minutes until reaching steady state. Then the packed-bed NTP reactor was activated by the selected high voltage supply. An electric vacuum pump (McMaster–Carr model #4176K11) was turned on to draw samples from the air stream near the inner wall of the pipe through the impingers (ACE Glass 7533-13) upstream and downstream of the reactor at 1 LPM, leading to collection of MS2 aerosols in the 20 ml impinger collection fluid (PBS).

For inactivation tests with the reactor powered by the 0–20 kV variable amplifier, the sampling time was 30 min. For tests with the 30 kV transformer, the sampling time was 60 min in order to collect a higher number of viable viruses within the impinger installed downstream of the reactor (figure 1). Virus samples were also collected directly from the ultrasonic humidifier reservoir before each trial. Plaque assays and reverse transcriptase quantitative polymerase chain reaction (RT-qPCR) assays, both described in detail below, were performed on each sample to determine the concentration of infectious MS2 plaque forming units (pfu/ml) and the concentration of MS2 genome copies (gc/ml) in the PBS collecting solution. To compare the humidifier reservoir samples with impinger samples, all of the acquired infectious MS2 concentrations in aqueous PBS solutions were converted to concentrations in the air stream using the following two mass balance equations:

$$C_{8,air} = \dot{V} \times \frac{C_3}{\dot{Q}_{air}} \quad (2)$$

$$C_{10,air} = \frac{V_{impinger} C_{10}}{\dot{Q}_{sample} t_{sample}}; C_{11,air} = \frac{V_{impinger} C_{11}}{\dot{Q}_{sample} t_{sample}} \quad (3)$$

where \dot{V} is the average ultrasonic atomization rate (117 ml h⁻¹), C_3 is the measured infective MS2 concentrations in samples acquired from the humidifier reservoir (position 3 in figure 1) immediately before each test. C_{10} and C_{11} are the infective MS2 concentrations in the impingers (positions 10 and 11 in figure 1 respectively). $C_{8,air}$, $C_{10,air}$ and $C_{11,air}$ are converted infectious MS2 concentrations in the airstream at the humidifier outlet and at the upstream and downstream sampling points, respectively. \dot{Q}_{air} is the air flow rate through the apparatus, $V_{impinger}$ is the volume of PBS in each of the impingers (20 ml), and \dot{Q}_{sample} and t_{sample} are, respectively, air flow rates through the impingers (1 LPM) and the standard elapsed time allowed for sampling (30 or 60 min). It should be noted that the MS2 inactivation in the reservoir during atomization is not considered in the calculation of $C_{8,air}$, so the calculated results should be good approximations rather than true values. According to our previous study, there may be a 0.3 log reduction of viable MS2 concentration in the humidifier reservoir during the 30 min test, but this inactivation would not affect the estimation of the NTP reactor inactivation efficiency as long as viable MS2 are measured in the upstream impinger [21]. Similarly, total virus genome concentrations (both infective and inactivated) were assessed with qPCR and measured as genome copies per milliliter of solution (gc/ml), corrected with equations (2) and (3), and reported as genome copies per liter of air.

MS2 propagation and enumeration. Bacteriophage MS2 (ATCC 15597-B1) and its corresponding *E. coli* host ATCC 15597 was purchased from American Type Culture Collection (ATCC). MS2 was propagated and assayed in its *E. coli* host using previously published methods [22, 23]. The virus stocks were purified using an Econo Fast Protein Liquid Chromatography system (Bio-Rad, USA) with a HiPrep Sephacryl S-400 HR column (GE, USA). The purified virus fractions were concentrated with 100 kDa Amicon ultracentrifugal filters (Millipore, USA), and finally filter-sterilized with 0.22 μ m PES membrane filters. The final MS2 stocks ($\sim 10^{11}$ pfu ml⁻¹) were stored in phosphate buffer (5 mM NaH₂PO₄ and 10 mM NaCl, pH 7.5) at 4 °C. In the experiments, the detection limit was 10 pfu ml⁻¹ since only 100 μ l of a sample was used for each plate.

RT-qPCR. Viral RNA was extracted from 200 μ l MS2 virus samples using Maxwell 16 Viral Total Nucleic Acid Purification Kits (Promega, Madison, WI) according to the manufacturer's instructions. Extracted RNA was eluted using 50 μ l of nuclease-free water. The forward primer (5'-CCGCTACCTT-GCCCTAAAC-3') and reverse primer (5'-GACGACAAC-CATGCCAAAC-3') were designed with the Primer3free software (<http://primer3.sourceforge.net/>) and purchased from ThermoFisher Scientific (Grand Island, NY). Extracted MS2 RNA samples and RNA standards were reverse transcribed and amplified in parallel in an Eppendorf Mastercycler ep realplex Real-time PCR System (Eppendorf, Hauppauge, NY). Each reverse transcription-qPCR reaction was run in 20 μ l of total volume comprising 10 μ l of GoTaq 1-Step Master Mix, 0.4 μ l of RT mix, 0.6 μ l each of 10 μ M forward and reverse primers, 6.4 μ l of nuclease-free water and 2 μ l of RNA sample (Promega, Madison, WI). The following thermocycling conditions were used: 15 min at 40 °C; 10 min at 95 °C; and 45 cycles of 95 °C for 15 s, 60 °C for 30 s and 72 °C for 40 s, followed by a melting ramp from 68 to 95 °C, with the temperature held for 45 s at 60 °C and for 5 s at all subsequent temperatures.

Measurements of system performance. During the experiment, a portable humidity/temperature pen (Traceable 4093) measured the temperature and relative humidity (RH) inside the sampling train upstream of the reactor. An insertable anemometer (Extech 407123) measured the air stream radial velocity profile ~ 30.5 cm (12-inch) downstream of the reactor. The pressure drops across the packed-bed NTP reactor and the ozone filter were measured by a low-pressure differential gauge (Magnehelic 2300-0). When the reactor was powered by the 0–20 kV variable amplifier, an oscilloscope (BK Precision Model-2190D) monitored the applied voltage and current to the packed-bed NTP reactor, from which the input and discharge power can be calculated. When the reactor was powered by the fixed 30 kV transformer, the total input power consumption of the transformer was measured by an electricity power meter (P3 International P4460), and the discharge power was measured by a high voltage probe and a Pearson coil, as discussed in the experimental setup section. To ensure that collected MS2 would not be inactivated in the impinger

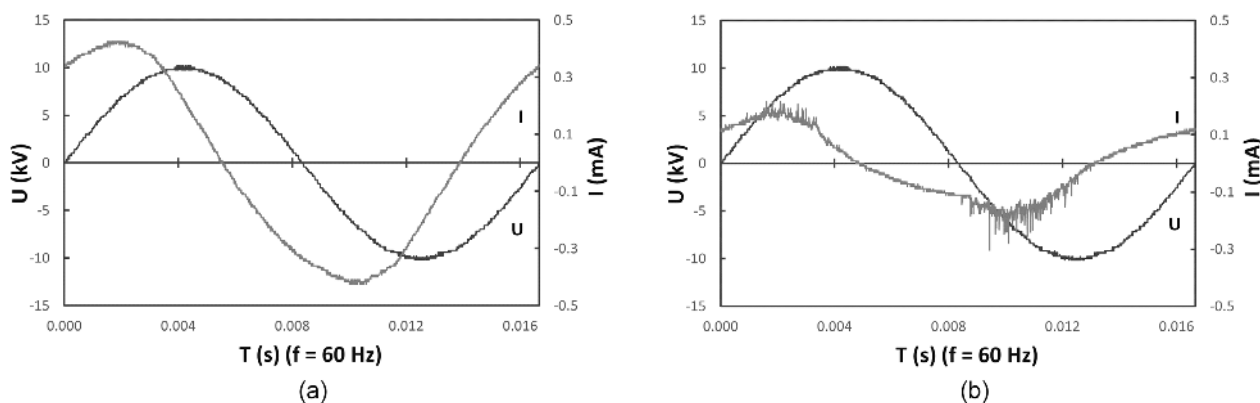


Figure 3. Applied voltage and (a) total current or (b) return current waveform acquired by the oscilloscope with 20kV peak-to-peak voltage.

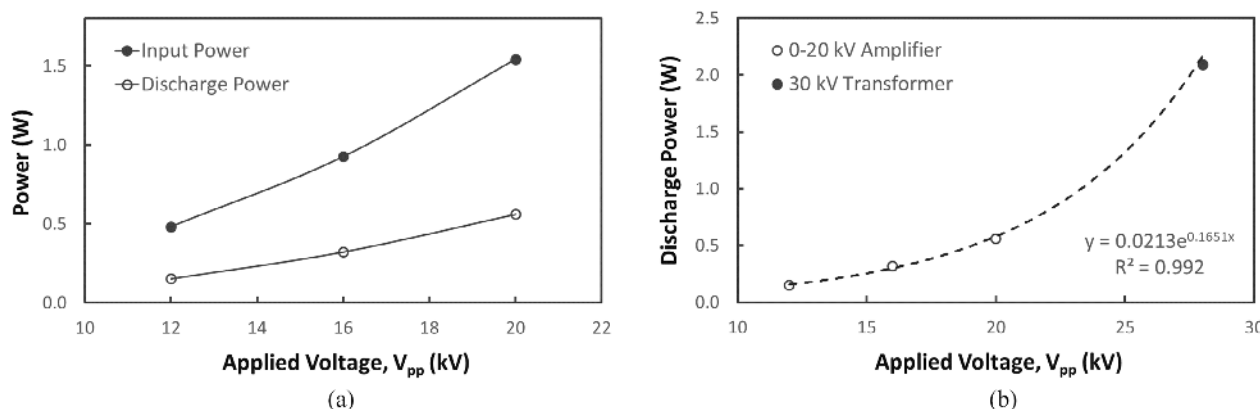


Figure 4. (a) Input and discharge power of the reactor at 12kV, 16kV and 20kV applied voltage with the 0–20kV variable amplifier; (b) estimated discharge power showed a strong exponential correlation with the applied voltage with both high voltage power supplies.

liquid during sampling, 20ml of 1×10^6 pfu ml⁻¹ MS2-PBS solution was added into the downstream impinger, which was then connected to the downstream sampling port. The packed-bed NTP reactor was either inactivated or activated by the 20kV voltage supply, and the effluent gas from the reactor was bubbled through the impinger liquid for 15, 30 and 45 min, after which the infectious MS2 concentrations in the impinger were assayed. Ozone generated by the packed-bed NTP reactor when energized had the potential to dissolve into sampling liquid in the downstream impinger and inactivate MS2 during and after sample collection. To quench the ozone in solution, 50 mM of anhydrous sodium sulfite (Na₂SO₃, Fisher Scientific BP355-500) was added into the downstream 20 ml impinger collection liquid. An ozone sensor (EcoSensors A-21ZX) measured the ozone concentration either upstream of the ozone filter (downstream of the reactor) or downstream of the filter to determine the amount of ozone generated by the packed-bed NTP reactor at various power and flow rate levels and to examine the removal efficiency of ozone by the ozone filter.

Results and discussion

Operating conditions

In this study, the overall air flow rate through the sampling train was estimated to be 170 LPM at 30% voltage setting

of the ID fan and 330 LPM at 60% voltage setting, by integrating the measured air velocity profile along the pipe radius. The pressure difference upstream and downstream of the NTP DBD packed bed measured at the 170 LPM flow rate was 45 Pa, a reasonably low difference due to the high porosity of the packed bed. The ozone filter was also quite porous, with a honeycomb structure that produced a pressure drop of 20 Pa at the flow rate of 170 LPM. The total pressure drop across the system was about 65 Pa at the flow rate of 170 LPM, or 0.38 Pa/LPM. It was estimated that at 170 LPM, the virus exposure time to NTP species was about 0.25 s.

Typical applied voltage and current waveforms measured by the oscilloscope are presented in figure 3, and all voltage and current waveforms at all voltage setups (12kV, 16kV, 20kV and 30kV) can be found in the supporting information. Two current waveforms were measured: the total current represented the current supplied into the system and was used to calculate input power; the return current represented the current returned to the supply from the ground electrode, and was used to calculate NTP discharge power. When applied voltage increased from 12kV to 20kV, the input power increased from 0.5 W to 1.5 W and the discharge power increased from 0.2 W to 0.6 W, 31%–36% of the input power (figure 4(a)). Kuwahara *et al* [12] reported similar differences (76%) between input and discharge power, and two other research reported that 20%–27% of the input power was converted to

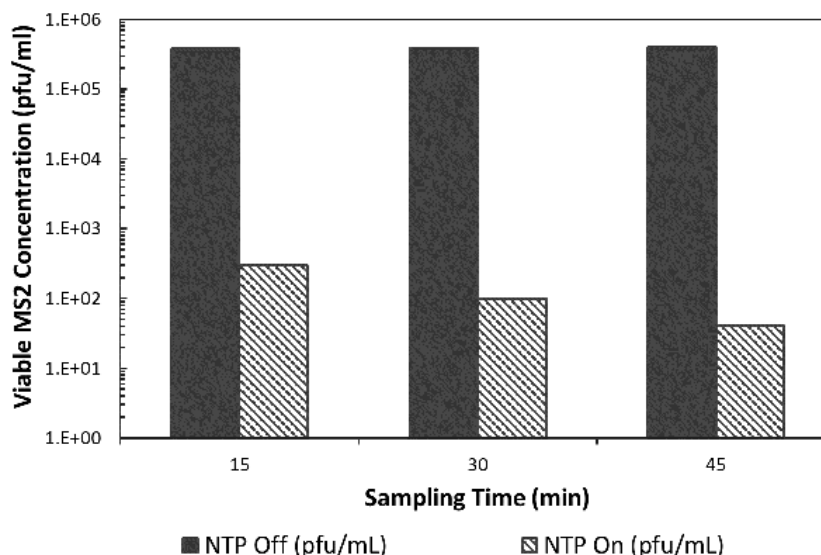


Figure 5. Change of infectious MS2 concentration in the downstream impinger with either ozone-free air (reactor off) or ozone-loaded air (reactor activated by 20kV) bubbling through the impinger liquid.

plasma discharge power in their NTP reactor [24, 25]. With the 0–20kV variable amplifier, the maximum discharge power in the reactor was 0.56 W (198 J m^{-3} at 170 LPM) at 20kV. With the fixed 30kV neon transformer, the actual peak-to-peak voltage applied to the reactor was 28kV and the total input power consumption was ~ 21 W measured by the commercial power meter. The estimated discharge power was 2.08 W (734 J m^{-3} at 170 LPM), 10% of the input power, according to the high voltage probe and Pearson coil measurements. The estimated discharge power showed a strong exponential correlation with the applied peak-to-peak voltage, no matter which power supply is used (figure 4(b)). In future, the V–Q Lissajous method can be applied to more accurately estimate the discharge power with both the 0–20kV variable amplifier and the 30kV neon transformer.

When ambient air was supplemented with dry compressed air, the initial temperature and RH of the air stream inside the sampling train were 20 °C and 30%, respectively. The addition of water mist from the humidifier into the air stream can induce evaporative cooling, in which the air temperature would be reduced, and the RH would be increased. According to the measurement data, at 170 LPM air flow rate and the humidifier power level 2 (H2; atomization rate of 117 ml h^{-1}), both the temperature and RH reached steady state values of 16.5 °C and 60%, respectively, after 30 min.

Control tests were conducted during which 20ml of an MS2 solution ($1 \times 10^6 \text{ pfu ml}^{-1}$ in PBS) was added into the downstream impinger and the effluent gas from the reactor was bubbled through the impinger liquid. The concentration of infective viruses when the NTP reactor was off proved that bubbling ozone-free air through the impinger for 45 min did not inactivate the MS2 (figure 5). When the reactor was on, a 3 log reduction in the infective MS2 concentration was observed in the impinger solution over the first 15 min. This indicated that when the reactor was activated by 20kV, the generated ozone dissolved in the impinger liquid and inactivated the sampled MS2. As the goal of these experiments was to inactivate viruses within the reactor and not in the sampling

liquid downstream of the reactor, the ozone that dissolved in the downstream impinger liquid was quenched with 50mM of anhydrous sodium sulfite. According to the measured ozone concentration and the calculated equilibrium dissolved ozone concentration in the impinger liquid (based on Henry's Law), the added sodium sulfite should be sufficient to quench all of the dissolved ozone during the packed-bed NTP inactivation tests. Control experiments proved that the sodium sulfite did not inactivate MS2 within the experimental timeframe.

MS2 Inactivation

The decrease in infective MS2 particles and total MS2 particles across the reactor were assayed by taking samples from the atomizer reservoir and samples from impingers both upstream and downstream of the NTP treatment. Although plaque assay results are normally reported in pfu per ml of solution and qPCR results are reported as gene copies (gc) per ml of solution, our reported concentrations are in pfu or gc per liter of air, which correspond to the overall air flow rate for the case of gross concentrations entering the sampling train, and to the 1 LPM air sampling rate through the impingers.

When the volumetric air flow rate was maintained at 170 LPM and the reactor was off, a ~ 2.6 log decrease in infective MS2 concentrations from the humidifier outlet to the upstream impinger was observed, as was a ~ 0.35 log decrease between the upstream and downstream impingers (figure 6). The qPCR results, which reflect the total number of viruses, suggested a decrease of ~ 1 log between the humidifier outlet and the upstream impinger and a decrease of ~ 0.35 log between the upstream and downstream impingers (figure 6). The ~ 1 log decrease in gene copy concentrations from the humidifier outlet (position 8) to the upstream impinger (position 10), which indicates the loss of total (infectious and inactivated) viruses during atomization, may have several causes, including wall losses along the four-meter-long duct. These impacts are discussed in greater detail in Xia *et al* [21]. The additional 1.6 log reduction in infectious MS2 concentrations

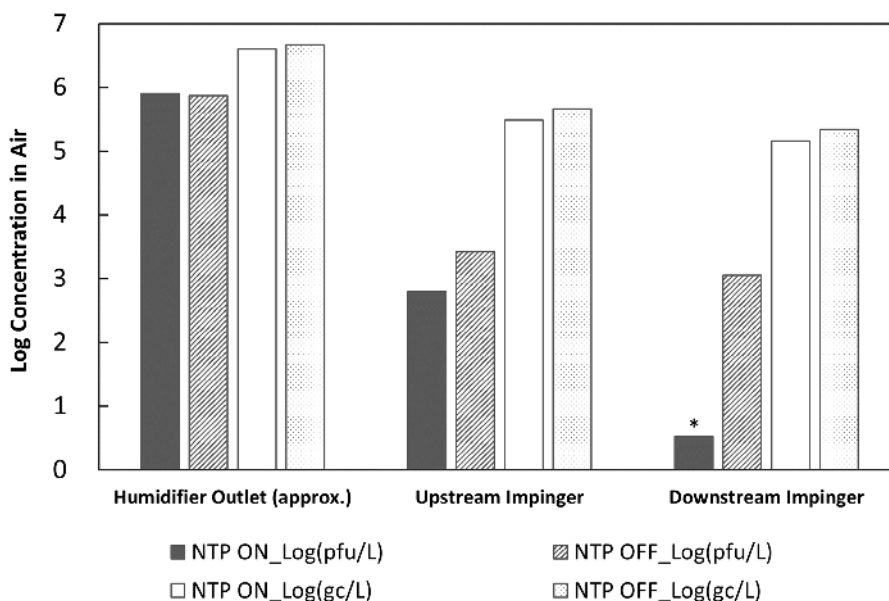


Figure 6. Concentrations of viruses in air measured with plaque assays and RT-qPCR in the NTP reactor powered by 30kV AC supply at a 170 LPM air flow rate (*: detection limit).

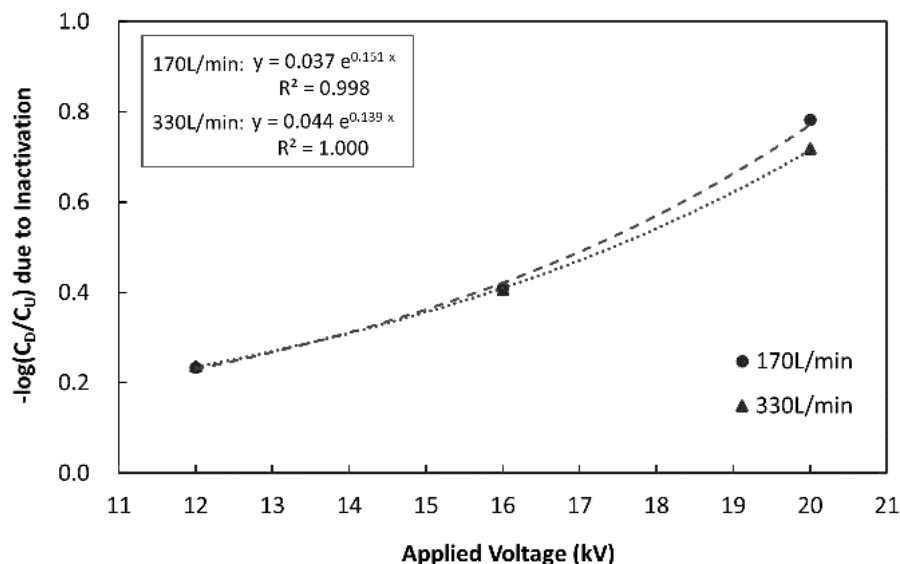


Figure 7. Log-reduction of infectious MS2 in airstream due to inactivation of the packed-bed NTP reactor activated by the variable voltage amplifier at 12kV, 16kV and 20kV (C_D and C_U represent the downstream and upstream concentrations in air, respectively).

was most likely caused by inactivation during the evaporation process of the atomized MS2-PBS droplets. Based on the qPCR results, the 0.35 log decrease of infectious viruses through the packed bed when the reactor was off was not due to inactivation of viruses in the aerosols and was likely due to physical filtration of the virus by the packed bed.

When the reactor was powered with the 30kV neon transformer, samples collected post-NTP treatment contained infective virus concentrations below our plaque assay limit of quantification (10 pfu ml^{-1}). Consequently, the reactor caused a decrease of more than 2.3 log infective MS2 (2 log inactivation if excluding the 0.35 log filtration discussed above) (figure 6). In contrast, the nearly constant reduction in gene copy concentrations with and without power to the reactor

suggests that the virus was inactivated, and not removed physically (figure 6). In Xia *et al* [21], we discuss the likely mechanisms responsible for the nearly three log reduction in infective MS2 concentration between the introduction of the aerosol at position 8 to the upstream impinger at position 10 (figure 1).

MS2 inactivation was measured over a range of lower voltages (12, 16, and 20kV) and two air flow rates (170 LPM and 330 LPM). Increasing the voltage resulted in an exponential increase in MS2 inactivation by the reactor (figure 7), when the packed-bed filtration effect (an average of 0.14 log) was subtracted. At an air flow rate of 170 LPM and 12kV, an infective virus inactivation reduction across the reactor of 0.23 log was observed. This increased to a 0.78 log reduction at

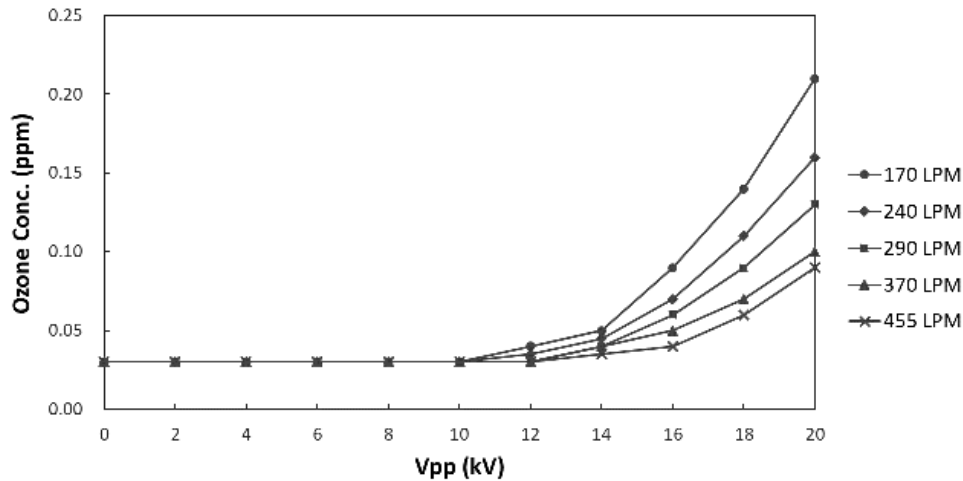


Figure 8. Measured ozone concentrations upstream of the ozone filter as a function of V_{pp} and air flow rate.

20 kV. Inactivation of infectious agents by chemical oxidants generally follows a Chick–Watson model, as illustrated by the equation below [26, 27]:

$$\ln\left(\frac{C_D}{C_U}\right) = -kC_{inact}^n t \quad (4)$$

where C_D and C_U are downstream and upstream infectious virus concentrations respectively, C_{inact} is the concentration of the inactivating agent generated by NTP, n is the coefficient of dilution (usually assumed to be 1), t is duration of treatment, and k is a kinetic constant. When the NTP reactor is operating at steady state under steady applied AC voltage, C_{inact} and treatment time t should remain constant. Increasing applied voltage to the NTP reactor increases the concentration of reactive ions and electrons (C_{inact}) in the plasma, and according to figure 7 and equation (4), C_{inact} should increase exponentially with increasing applied voltage. This assertion, however, needs to be justified in future plasma species measurements and analysis. Increasing the flow rate to 330 LPM, and consequently reducing the treatment time by approximately 50%, had a small impact on inactivation (figure 7), which indicates that the amount of treated air by the reactor can be increased without having a major impact on inactivation efficiency. This may be because that the predominant species inactivating aerosolized MS2 in this study were short-lived radicals rather than long-lived ozone, whose lifetime is at the scale of nanoseconds [28] and would not be affected by the change of second-scale exposure time. Wu *et al* [18] reported similar limited impact of treatment time on NTP inactivation efficiency. Specifically, the study showed that doubling the treatment time would only cause a 2%–4% further inactivation of waterborne MS2 by plasma gas. Extrapolating the results obtained at 12–20 kV and 170 LPM to 30 kV according to the trendline would yield an estimated 3.5 log reduction, in agreement with the greater than 2 log reduction obtained with the fixed 30 kV neon transformer.

In this study, at the flow rate of 170 LPM, the virus exposure time to NTP species was about 0.25 s, and the steady state ozone concentration downstream of the reactor was measured as 0.21 ppm at 20 kV and 2.08 ppm at 30 kV. The ozone

dose received by aerosolized MS2 was thereby estimated as $0.0017 \text{ min mg m}^{-3}$ at 20 kV and $0.017 \text{ min mg m}^{-3}$ at 30 kV (assuming room temperature and pressure). According to Tseng and Li [29], 90% (1 log) inactivation of airborne MS2 required an ozone dose of $1.28 \text{ min mg m}^{-3}$, which is 75–750 times of the ozone dose provided in this study. It was therefore concluded that ozone acted as a secondary inactivating reagent in this study and that aerosolized MS2 was predominantly inactivated by radicals and other reactive oxygen species (ROS) generated by the packed-bed NTP reactor over the short exposure time.

Our MS2 inactivation results (figures 6 and 7) are comparable with the previous studies. For example, Vaze *et al* applied 28 kV 600 μs pulse discharges to generate NTP, and the reactor achieved 97% inactivation of *E. coli* (1.5 log reduction) during the 10 s treatment time [17]. When the plasma generation area was reduced by 25%, the reactor's *E. coli* inactivation efficiency reduced significantly to 29% (0.16 log reduction) [19]. Wu *et al* applied a 14 kV 10 kHz AC power supply, and at 20 W power level, the reactor achieved ~80% MS2 inactivation (0.9 log reduction) in room air during a 0.12 s treatment time [18]. Both of these studies, however, only reported the reductions of viable bioaerosol concentration after the NTP treatment, and did not separate the inactivation effect of the active plasma species from the physical electrostatic precipitation or filtering effect of the reactor.

Ozone generation by the NTP reactor

One major concern for NTP-based airstream disinfection is the production of ozone in ventilation air, which can have detrimental impacts on human and animal health [30]. In California, state environmental regulations [31] require that indoor air cleaning devices intended for use in occupied spaces should not produce ozone concentrations greater than 0.05 ppm in treated air streams. We therefore adapted consumer-grade activated carbon honeycomb filters, normally installed over exhaust vents of photocopiers and laser printers, for use as a post-NTP treatment ozone filter.

The ozone concentrations were measured in the airstream upstream of the ozone filter (downstream of the packed bed

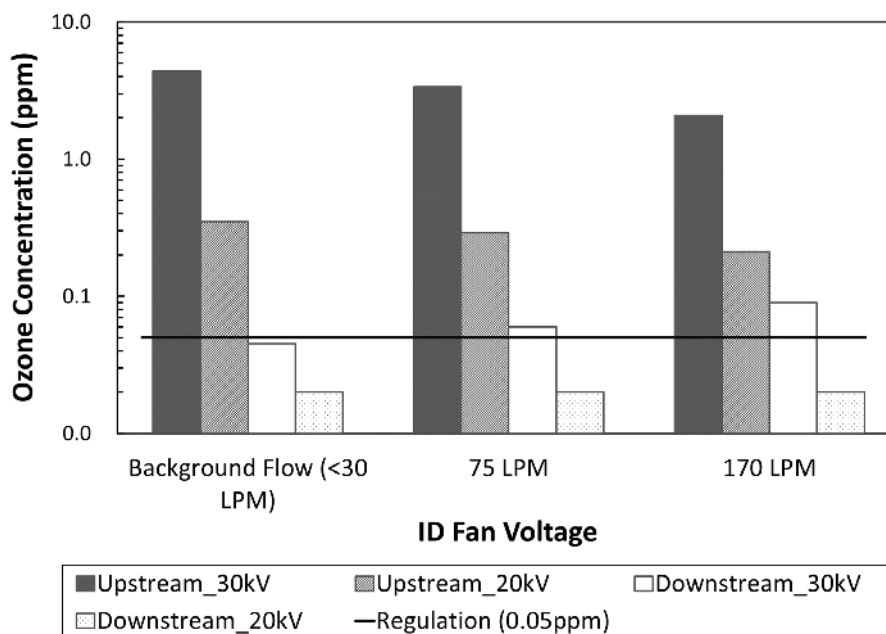


Figure 9. Measured ozone concentration upstream and downstream of the single layer ozone filter with either 20kV or 30kV power supply at varied air flow rates. The dashed line represents the ozone standard for indoor air cleaners set by the state of California [31].

section of the reactor), as a function of peak-to-peak voltage (V_{pp}) applied by the Trek high voltage power supply (figure 8). The baseline ozone concentration in the room air was 0.03 ppm. Results suggest that plasma was not established in the reactor and no ozone was produced until the applied V_{pp} exceeded 10kV (figure 8). Above 10kV, the ozone concentration downstream of the packed bed and upstream of the ozone filter increased with increasing V_{pp} and decreased due to reduction of NTP discharge energy density (discharge energy per unit volume of the air flow) with increasing air flow rate, as set by the ID fan. When 20kV AC voltage was applied to the packed-bed NTP reactor and at the 170 LPM flow rate, the highest ozone concentration downstream of the reactor was 0.21 ppm.

Ozone concentrations were measured upstream and downstream of a single, centimeter-thick ozone filter under reactor-on conditions at 20kV (discharge power of 0.56 W) and 30kV (discharge power of 2.08 W) over a range of air flow rates (figure 9). Increasing air flow rates corresponded with decreasing upstream ozone concentrations due to reduction of NTP discharge energy density, and increasing downstream ozone concentrations, likely due to increasing space velocity (defined as volumetric flow rate normalized by filter volume) and thus decreasing filter performance. The much higher supplied power of the 30kV power supply, as compared to the 20kV power supply, also produced more ozone, approximately ten times higher at all three flow rate conditions (figure 9). This was likely a result of greater oxygen atom radical (O) production at the higher power, which reacted with the available O_2 to form more O_3 [32, 33]. At 170 LPM and 30kV, the single layer of the activated carbon filter reduced upstream ozone concentrations by 96%; however, the downstream O_3 concentration (0.09 ppm) still exceeded the 0.05 ppm California standard. The addition of

a second filter would very likely reduce concentrations below the California standard, with little increase in the pressure drop across the filter (20 Pa at the flow rate of 170 LPM).

Conclusion

In this study, we successfully designed and constructed a packed-bed DBD NTP reactor that was effective at inactivating bacteriophage MS2 in aerosols with minimal pressure drop across the reactor. Ozone generated by the active plasma was effectively reduced to meet regulation standards by the insertion of commercial ozone filters without significant pressure drop. In future applications, the packed-bed depth, the dielectric material, and the air flow rate through the sampling train can be modified to achieve improved performance at various flow conditions.

Associated content

Acknowledgment

This article is based upon work that is supported by the National Institute of Food and Agriculture, US Department of Agriculture, under Award No. 2016-67030-24892. Any opinions, findings, conclusions, or recommendations expressed in this publication are those of the author(s) and do not necessarily reflect the view of the US Department of Agriculture. The authors thank Minmeng Tang and Yinyin Ye (University of Michigan) for helping in the experimental setup and plaque assay analysis respectively. The authors also thank Professor John Foster and Selman Mujovic (University of Michigan) for helping in the design and power consumption measurements of the packed-bed NTP reactor used in this research.

Supporting information

Please see the supplementary material document, available online.

Author contributions

The manuscript was written through contributions from all authors. All authors have given approval to the final version of the manuscript.

Funding sources

This article is based upon work that is supported by the National Institute of Food and Agriculture, US Department of Agriculture, under Award No. 2016-67030-24892.

Notes

E M L and H L C are affiliated with Taza Aya LLC; H L C is co-founder and CEO. T X, A K, Z Q, and K R W all declare no competing financial interest.

ORCID iDs

T Xia  <https://orcid.org/0000-0002-0601-0467>

References

- [1] McKinney K R, Gong Y Y and Lewis T G 2006 Environmental transmission of SARS at Amoy Gardens *J. Environ. Health* **68** 26
- [2] Hermann J, Hoff S, Muñoz-Zanzi C, Yoon K-J, Roof M, Burkhardt A and Zimmerman J 2007 Effect of temperature and relative humidity on the stability of infectious porcine reproductive and respiratory syndrome virus in aerosols *Vet. Res.* **38** 81–93
- [3] Ostfeld R S 2009 Climate change and the distribution and intensity of infectious diseases *Ecology* **90** 903–5
- [4] Kowalski W J, Bahnfleth W P, Witham D L, Severin B F and Whittam T S 2000 Mathematical modeling of ultraviolet germicidal irradiation for air disinfection *Quant. Microbiol.* **2** 249–70
- [5] Riley R L 1961 Airborne pulmonary tuberculosis *Bacteriol. Rev.* **25** 243
- [6] Wheeler S M, Ingraham H S, Hollaneder A, Lill N D, Gershon-Cohen J and Brown E W 1945 Ultra-violet light control of air-borne infections in a naval training center: preliminary report *Am. J. Public Health Nation's Health* **35** 457–68
- [7] Memarzadeh F, Olmsted R N and Bartley J M 2010 Applications of ultraviolet germicidal irradiation disinfection in health care facilities: effective adjunct, but not stand-alone technology *Am. J. Infect. Control* **38** S13–24
- [8] USEPA 2018 *Air Cleaners and Air Filters in the Home* (Washington, DC: EPA Office of Radiation and Indoor Air, Indoor Environments Division)
- [9] Pitkin A, Deen J and Dee S 2009 Use of a production region model to assess the airborne spread of porcine reproductive and respiratory syndrome virus *Vet. Microbiol.* **136** 1–7
- [10] Kim H H 2004 Nonthermal plasma processing for air-pollution control: a historical review, current issues, and future prospects *Plasma Process. Polym.* **1** 91–110
- [11] Holzer F, Kopinke F and Roland U 2005 Influence of ferroelectric materials and catalysts on the performance of non-thermal plasma (NTP) for the removal of air pollutants *Plasma Chem. Plasma Process.* **25** 595–611
- [12] Kuwahara T, Okubo M, Kuroki T, Kametaka H and Yamamoto T 2011 Odor removal characteristics of a laminated film-electrode packed-bed nonthermal plasma reactor *Sensors* **11** 5529–42
- [13] Park S S, Kang M S and Hwang J 2015 Oil mist collection and oil mist-to-gas conversion via dielectric barrier discharge at atmospheric pressure *Sep. Purif. Technol.* **151** 324–31
- [14] Vandenbroucke A M, Morent R, De Geyter N and Leys C 2011 Non-thermal plasmas for non-catalytic and catalytic VOC abatement *J. Hazard. Mater.* **195** 30–54
- [15] Mizuno A, Yamazaki Y, Ito H and Yoshida H 1989 AC energized ferroelectric pellet bed precipitator for sterilization and gas clean up *IEEE Industry Applications Society Annual Meeting* pp 2148–53
- [16] Mizuno A, Yamazaki Y, Ito H and Yoshida H 1992 AC energized ferroelectric pellet bed gas cleaner *IEEE Trans. Ind. Appl.* **28** 535–40
- [17] Vaze N D, Arjunan K P, Gallagher M J, Vasilets V N, Gutsol A, Fridman A and Anandan S 2007 Air and water sterilization using non-thermal plasma *16th IEEE Int. Pulsed Power Conf. (IEEE)* pp 1231–5
- [18] Wu Y, Liang Y, Wei K, Li W, Yao M, Zhang J and Grinshpun S A 2015 MS2 virus inactivation by atmospheric-pressure cold plasma using different gas carriers and power levels *Appl. Environ. Microbiol.* **81** 996–1002
- [19] Vaze N D, Gallagher M J, Park S, Fridman G, Vasilets V N, Gutsol A F, Anandan S, Friedman G and Fridman A A 2010 Inactivation of bacteria in flight by direct exposure to nonthermal plasma *IEEE Trans. Plasma Sci.* **38** 3234–40
- [20] Liang Y, Wu Y, Sun K, Chen Q, Shen F, Zhang J, Yao M, Zhu T and Fang J 2012 Rapid inactivation of biological species in the air using atmospheric pressure nonthermal plasma *Environ. Sci. Technol.* **46** 3360–8
- [21] Xia T, Kleinheksel A, Wigginton K R and Clack H L 2019 Suspending viruses in an airstream using a consumer-grade ultrasonic humidifier *Aerosol Sci. Technol.* in preparation
- [22] Pecson B M, Martin L V and Kohn T 2009 Quantitative PCR for determining the infectivity of bacteriophage MS2 upon inactivation by heat, UV-B radiation, and singlet oxygen: Advantages and limitations of an enzymatic treatment to reduce false-positive results *Appl. Environ. Microbiol.* **75** 5544–54
- [23] United States Environmental Protection Agency 2001 *Environmental Protection Agency Method 1601: Male-Specific (f+) and Somatic Coliphage in Water by Two-Step* (Washington, DC: US EPA Office of Water)
- [24] Harling A M, Glover D J, Whitehead J C and Zhang K 2009 The role of ozone in the plasma-catalytic destruction of environmental pollutants *Appl. Catal. B* **90** 157–61
- [25] Ogata A, Mizuno K, Kushiyama S and Yamamoto T 1998 Methane decomposition in a barium titanate packed-bed nonthermal plasma reactor *Plasma Chem. Plasma Process.* **18** 363–73
- [26] Chick H 1908 An investigation of the laws of disinfection *J. Hygiene* **8** 92–158
- [27] Watson H 1908 A note on the variation of the rate of disinfection with change in the concentration of the disinfectant *J. Hygiene* **8** 536–42

- [28] Eliasson B and Kogelschatz U 1991 Nonequilibrium volume plasma chemical processing *IEEE Trans. Plasma Sci.* **19** 1063–77
- [29] Tseng C-C and Li C-S 2006 Ozone for inactivation of aerosolized bacteriophages *Aerosol Sci. Technol.* **40** 683–9
- [30] Lippmann M 1989 Health effects of ozone. A critical review *JAPCA* **39** 672–95
- [31] Jakober C and Phillips T 2008 *Evaluation of Ozone Emissions From Portable Indoor Air Cleaners: Electrostatic Precipitators and Ionizers* (Sacramento, CA: California Environmental Protection Agency, Air Resources Board)
- [32] Yehia A and Mizuno A 2013 Ozone generation by negative direct current corona discharges in dry air fed coaxial wire-cylinder reactors *J. Appl. Phys.* **113** 183301
- [33] Penetrante B, Hsiao M, Bardsley J, Merritt B, Vogtlin G, Kuthi A, Burkhart C and Bayless J 1997 Identification of mechanisms for decomposition of air pollutants by non-thermal plasma processing *Plasma Sources Sci. Technol.* **6** 251–9